

Decentralized Beamforming Design for Intelligent Reflecting Surface-Enhanced Cell-Free Networks

Shaocheng Huang^{ID}, Yu Ye^{ID}, *Student Member, IEEE*, Ming Xiao^{ID}, *Senior Member, IEEE*,
H. Vincent Poor^{ID}, *Life Fellow, IEEE*, and Mikael Skoglund^{ID}, *Fellow, IEEE*

Abstract—Cell-free networks are considered to be a promising distributed network architecture to satisfy the increasing number of users and high rate expectations in beyond-5G systems. However, to further enhance network capacity, an increasing number of high-cost base stations (BSs) is required. To address this problem and inspired by the cost-effective intelligent reflecting surface (IRS) technique, we propose a fully decentralized design framework for cooperative beamforming in IRS-aided cell-free networks. We first transform the centralized weighted sum-rate maximization problem into a tractable consensus optimization problem, and then an incremental alternating direction method of multipliers (ADMM) algorithm is proposed to locally update the beamformer. The complexity and convergence of the proposed method are analyzed, and these results show that the performance of the new scheme can asymptotically approach that of the centralized one as the number of iterations increases. Results also show that IRSs can significantly increase the system sum-rate of cell-free networks and the proposed method outperforms existing decentralized methods.

Index Terms—Beamforming, cell-free networks, intelligent reflecting surface, decentralized optimization.

I. INTRODUCTION

RECENTLY, a user-centric network paradigm called cell-free networks has been considered as a promising technique to provide high network capacity and overcome the cell-boundary effect of traditional network-centric networks (e.g., cellular networks) [1]–[4]. In cell-free networks, a large number of distributed service antennas, which are connected to central processing units (CPUs), coherently serve all users on the same time-frequency resource [2]. This distributed communication network can offer many degrees of freedom and high

multiplexing gain. Recent results show that cell-free networks outperform traditional cellular and small-cell networks in several practical scenarios [2], [3]. To provide high directional gains, beamforming design is important in cell-free networks. To cooperatively design beamforming, a centralized zero-forcing (ZF) beamforming scheme is proposed in [5]. Since the CPU should collect all instantaneous channel state information (CSI) of all base stations (BSs), centralized approaches might be unsalable when the number of BSs and users (UEs) is large and the beamforming optimization at the CPU may be overwhelming due to the high dimensionality of aggregated beamformers. To avoid instantaneous CSI exchange among BSs via backhauling and reduce computation complexity at CPU, most recent works assume a simple non-cooperative beamforming strategy at the BSs, e.g., maximum ratio transmission (MRT) [3] and local ZF [4]. However, cooperation among BSs is not considered, and thus interference among BSs cannot be efficiently eliminated. Though a distributed beamforming scheme is introduced in [6], it is not fully decentralized and each local update requires extensive CSI exchange among BSs.

To further increase the capacity of cell-free networks, the deployment of more distributed BSs requires high hardware cost and power consumption [3]. Moreover, when a cell-free network implemented at high-frequency bands (e.g., millimeter-wave bands), it might suffer severe propagation loss and be vulnerable to blockage [7]. Meanwhile, an emerging technique called intelligent reflecting surface (IRS) equipped with low-cost, energy-efficient and high-gain meta-surfaces can potentially address the above problems [8]–[10]. In [8], it is shown that the IRS outperforms decode-and-forward relaying if the size of the IRS is large. In addition, a centralized beamforming scheme of cell-free networks is proposed in [10], in which a part of BSs in the network is replaced by IRSs to improve the network capacity at low cost and power consumption. It is shown that the cell-free network with IRSs can achieve a larger weighted sum-rate (WSR) than that without IRSs. However, there is no decentralized beamforming scheme for IRS-aided cell-free networks.

Based on above observations, we first propose a decentralized design framework for cooperative beamforming in IRS-aided cell-free networks, in which transmitting digital beamformers and IRS-based analog beamformers are jointly optimized. Specifically, we equivalently transform the untractable centralized beamforming optimization problem to a tractable decentralized optimization problem based on recent fractional programming (FP). Then, we derive the closed-form explanation of each updating variable and propose a fully decentralized beamforming scheme based on the alternating direction method of multipliers (ADMM) to incrementally and locally update the beamformers. Since only three variables are incrementally updated and transmitted to the next

Manuscript received September 11, 2020; revised November 13, 2020; accepted December 9, 2020. Date of publication December 18, 2020; date of current version March 9, 2021. The work of Ming Xiao was supported in part by EU Marie Skłodowska-Curie Actions Project entitled “High-Reliability Low-Latency Communications With Network Coding”; in part by ERA-NET Smart Energy Systems SG+ 2017 Program, “SMART-MLA” under Project 89029 (SWEA number 42811-2); Swedish Strategic Research Foundation Project “High-Reliable Low-Latency Industrial Wireless Communications”; and in part by Swedish Foundation for International Cooperation in Research and Higher Education (STINT), Project “Efficient and Secure Distributed Machine Learning with Gradient Descent.” The work of H. Vincent Poor was supported in part by the U.S. National Science Foundation under Grant CCF-1908308. The associate editor coordinating the review of this article and approving it for publication was K. Rabie. (Corresponding author: Ming Xiao.)

Shaocheng Huang, Yu Ye, Ming Xiao, and Mikael Skoglund are with the School of Electrical Engineering and Computer Science, KTH Royal Institute of Technology, 100 44 Stockholm, Sweden (e-mail: shahua@kth.se; yu9@kth.se; mingx@kth.se; skoglund@kth.se).

H. Vincent Poor is with the Department of Electrical Engineering, Princeton University, Princeton, NJ 08544 USA (e-mail: poor@princeton.edu).

Digital Object Identifier 10.1109/LWC.2020.3045884

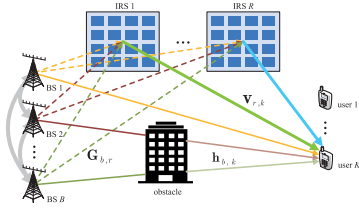


Fig. 1. IRS-aided cell-free networks.

BS, our scheme can significantly reduce backhaul signaling compared with full CSI exchange among BSs. Further, a low-complexity majorization-minimization (MM) method is proposed to efficiently optimize the IRS-based analog beamformer with non-convex constraints. Results show that the MM method can achieve comparable performance to the semidefinite relaxation (SDR) method. The convergence of the decentralized method has been proven and the main complexity has been analyzed.

II. SYSTEM MODEL

We consider a downlink RIS-aided cell-free system, as shown in Fig. 1, where a set of BSs $\mathcal{B} = \{1, \dots, B\}$ and a set of IRSs $\mathcal{R} = \{1, \dots, R\}$ serve a set of UEs $\mathcal{K} = \{1, \dots, K\}$. Let the number of antennas equipped at each BS and UE be N_t and 1, respectively, and the number of reflection elements at each RIS be N . With the reflection support of IRSs, the channel between each BS and each UE consists of two parts: the BS-UE link and R BS-IRS-UE links, where each BS-IRS-UE link is modeled as a concatenation of three components, i.e., the BS-IRS link, IRS phase-shift matrix, and IRS-UE link [10]. Thus, the equivalent channel between the b -th BS and the k -th UE is modeled as

$$\hat{\mathbf{h}}_{b,k}^H = \mathbf{h}_{b,k}^H + \sum_{r \in \mathcal{R}} \mathbf{v}_{r,k}^H \boldsymbol{\Theta}_r^H \mathbf{G}_{b,r} \quad (1a)$$

$$= \mathbf{h}_{b,k}^H + \boldsymbol{\theta}^H \mathbf{V}_k^H \mathbf{G}_b, \quad (1b)$$

where $\mathbf{h}_{b,k} \in \mathbb{C}^{N_t}$, $\mathbf{v}_{r,k} \in \mathbb{C}^N$ and $\mathbf{G}_{b,r} \in \mathbb{C}^{N \times N_t}$ denote the channel from the b -th BS to the k -th UE, from the r -th IRS to the k -th UE, and from the b -th BS to the r -th IRS, respectively. $\boldsymbol{\Theta}_r = \text{diag}(\theta_{r,1}, \dots, \theta_{r,N}) \in \mathbb{C}^{N \times N}$ denotes the phase shift matrix at the r -th IRS, where $|\theta_{r,n}|^2 = 1, \forall r, n$ [9]. The equivalent channel can be compactly expressed as (1b) by defining $\mathbf{V}_k = \text{diag}([\mathbf{v}_{1,k}^T, \dots, \mathbf{v}_{R,k}^T]) \in \mathbb{C}^{NR \times NR}$, $\mathbf{G}_b = [\mathbf{G}_{b,1}^T, \dots, \mathbf{G}_{b,R}^T] \in \mathbb{C}^{NR \times N_t}$, $\boldsymbol{\theta} = \Delta \mathbf{1}_{NR}$ and $\Delta = \text{diag}(\boldsymbol{\Theta}_1, \dots, \boldsymbol{\Theta}_R) \in \mathbb{C}^{NR \times NR}$. Then, the IRS constraints can be defined as $\boldsymbol{\theta} \in \mathcal{F}$, where \mathcal{F} is the set of NR -dimensional vectors of unit-modulus entries. Let $s_k \sim \mathcal{CN}(0, 1)$ denote the transmitted symbol to UE k . Likewise, let $\mathbf{w}_b = [\mathbf{w}_{b,1}^T, \dots, \mathbf{w}_{b,K}^T]^T$, where $\mathbf{w}_{b,k} \in \mathbb{C}^{N_t}$ is the precoding vector used by BS b for UE k . We assume the per-BS power constraint $\sum_{k \in \mathcal{K}} \|\mathbf{w}_{b,k}\|^2 \leq P_b, \forall b$, where P_b denotes the maximum transmit power at BS b . Thus, the received signal at the k -th UE is $y_k = \sum_{b \in \mathcal{B}} \sum_{j \in \mathcal{K}} \hat{\mathbf{h}}_{b,k}^H \mathbf{w}_{b,j} s_j + z_k$ where $z_k \sim \mathcal{CN}(0, \delta^2)$ is average Gaussian noise at UE k . Then, the signal-to-interference-plus-noise (SINR) at UE k is

$$\Gamma_k = \frac{|\sum_{b \in \mathcal{B}} \hat{\mathbf{h}}_{b,k}^H \mathbf{w}_{b,k}|^2}{\sum_{j \in \mathcal{K}, j \neq k} |\sum_{b \in \mathcal{B}} \hat{\mathbf{h}}_{b,k}^H \mathbf{w}_{b,j}|^2 + \delta^2}. \quad (2)$$

Our objective is to maximize the WSR of all K UEs by jointly designing transmitting digital beamformers and IRS-based analog beamformers, subject to per-BS transmit power constraints and phase shift constraints. Thus, the centralized WSR maximization problem is formulated as

$$\begin{aligned} (\text{P1}) : \max_{\boldsymbol{\theta}, \mathbf{W}} R_s &= \sum_{k \in \mathcal{K}} \omega_k \log(1 + \Gamma_k) \\ \text{s. t. } \sum_{k \in \mathcal{K}} \|\mathbf{w}_{b,k}\|^2 &\leq P_b, b \in \mathcal{B}; \boldsymbol{\theta} \in \mathcal{F}, \end{aligned} \quad (3)$$

where $\mathbf{W} = \{\mathbf{w}_b | b \in \mathcal{B}\}$. To characterize the theoretical performance gain with the IRS, we assume that perfect channel state information is available at the BS, which can be obtained based on existing channel estimation schemes such as [9], [11]. Based on the letter in [11] and with the received uplink pilot sequences from UEs over multiple sub-phases, the BS can perfectly estimate the direct channel (i.e., $\mathbf{h}_{b,k}$) and the cascaded IRS channel (i.e., $\mathbf{G}_b^H \mathbf{V}_k$) with least squares estimations when the training overhead (user transmit power) is sufficiently large. Then the BS is responsible for optimizing the IRS phase shifts and sending them back to the IRS controller through wired or wireless links [10].

III. DECENTRALIZED BEAMFORMING DESIGN

In what follows, we will propose a fully decentralized beamforming scheme to solve problem (P1), where information is exchanged only among neighboring BSs via backhaul signaling and BS-specific beamformers are computed locally by the BSs.

Under decentralized processing, the IRS-based analog beamformer computed by each BS should reach consensus. That is, we should guarantee $\boldsymbol{\theta}_b = \boldsymbol{\theta}_l, b \in \mathcal{B}$ and $l \in \mathcal{B} \setminus b$, where $\boldsymbol{\theta}_b$ is the local IRS-based analog beamformer computed at BS b . On the other hand, the WSR maximization problem (P1) is non-convex w.r.t. $\boldsymbol{\theta}_b$ and \mathbf{w}_b due to the coupled variables in the ratio term of WSR in (3) and the constant modulus constraints of phase shift vectors. Therefore, we first transform problem (P1) to a tractable problem based on the Lagrangian dual transform and fractional programming theory [12]. By introducing two auxiliary variables $\boldsymbol{\gamma} = [\gamma_1, \dots, \gamma_K] \in \mathbb{R}^K$ and $\boldsymbol{\xi} = [\xi_1, \dots, \xi_K] \in \mathbb{C}^K$, problem (P1) can be equivalently rewritten as

$$\begin{aligned} (\text{P2}) : \min_{\boldsymbol{\theta}, \mathbf{W}} f(\boldsymbol{\theta}, \mathbf{W}, \boldsymbol{\gamma}, \boldsymbol{\xi}) \\ \text{s. t. } \sum_{k \in \mathcal{K}} \|\mathbf{w}_{b,k}\|^2 &\leq P_b, b \in \mathcal{B}; \\ \boldsymbol{\theta}_b &= \boldsymbol{\theta}_l, b \in \mathcal{B}, l \in \mathcal{B} \setminus b; \boldsymbol{\theta}_b \in \mathcal{F}, b \in \mathcal{B}, \end{aligned} \quad (4)$$

where $\boldsymbol{\theta} = \{\boldsymbol{\theta}_b | b \in \mathcal{B}\}$,

$$\begin{aligned} f(\boldsymbol{\theta}, \mathbf{W}, \boldsymbol{\gamma}, \boldsymbol{\xi}) &= \sum_{k \in \mathcal{K}} \omega_k \left(\sum_{j \in \mathcal{K}} |\xi_j|^2 \left| \sum_{b \in \mathcal{B}} \hat{\mathbf{h}}_{b,j}^H \mathbf{w}_{b,k} \right|^2 \right. \\ &\quad \left. - 2\sqrt{1 + \gamma_k} \sum_{b \in \mathcal{B}} \text{Re}\{\xi_k^* \hat{\mathbf{h}}_{b,k}^H \mathbf{w}_{b,k}\} \right. \\ &\quad \left. - \log(1 + \gamma_k) + \gamma_k + |\xi_k|^2 \delta^2 \right). \end{aligned} \quad (5)$$

For the detailed transformation of problem (P2), the reader is referred to [12]. Note that problem (P2) is a consensus optimization problem w.r.t. $\boldsymbol{\theta}_b, \forall b$. Meanwhile, problem (P2)

is a bi-convex optimization problem with fixing Θ and a common practice for solving it is the alternative optimization method. To compactly expressed the consensus constraint in problem (P2), we let $\mathcal{G} = \{\mathcal{B}, \mathcal{E}\}$ denote an undirected graph where \mathcal{B} is the BSs and \mathcal{E} includes the connections. Let $e \in \{1, \dots, |\mathcal{E}|\}$ and $\mathbf{A} = [\mathbf{A}_1, \dots, \mathbf{A}_B]$ be composed of $|\mathcal{E}|B$ blocks of $NR \times NR$ matrices with $\mathbf{A}_b \in \mathbb{R}^{NR|\mathcal{E}| \times NR}$. Then, the consensus constraint w.r.t. $\theta_b, \forall b$, can be reformulated as $\mathbf{t} = \sum_{b \in \mathcal{B}} \mathbf{A}_b \theta_b = \mathbf{0}$ where \mathbf{A} is deduced from: if $(b, l) = \mathcal{E}_e, \forall b, l$, the (e, b) -th block and the (e, l) -th block of \mathbf{A} are respectively \mathbf{I}_{NR} and $-\mathbf{I}_{NR}$; otherwise the corresponding blocks are zero matrices $\mathbf{0}_{NR}$. To effectively solve problem (P2), we then utilize the ADMM method in [13], [14]. The augmented Lagrangian for problem (P2) is

$$\begin{aligned} \mathcal{L}(\Theta, \mathbf{W}, \boldsymbol{\gamma}, \boldsymbol{\xi}, \boldsymbol{\lambda}) = & f(\Theta, \mathbf{W}, \boldsymbol{\gamma}, \boldsymbol{\xi}) + \sum_{b \in \mathcal{B}} \mu_b \left(\sum_{k \in \mathcal{K}} \|\mathbf{w}_{b,k}\|^2 - P_b \right) \\ & + \sum_{b \in \mathcal{B}} \mathbb{1}_{\mathcal{F}}(\theta_b) + \frac{\rho}{2} \left\| \sum_{b \in \mathcal{B}} \mathbf{A}_b \theta_b + \frac{\boldsymbol{\lambda}}{\rho} \right\|^2, \quad (6) \end{aligned}$$

where $\boldsymbol{\lambda}$ is a Lagrange multiplier and $\rho > 0$, $\mu_b, \forall b$, is the dual variable introduced for each per-BS power constraints, $\mathbb{1}_{\mathcal{F}}(\cdot)$ is the indicator function of set \mathcal{F} (i.e., $\mathbb{1}_{\mathcal{F}}(\theta_b) = 0$ if $\theta_b \in \mathcal{F}$; otherwise, $\mathbb{1}_{\mathcal{F}}(\theta_b) = +\infty$).

Since the incremental update method for decentralized optimization is more communication-efficient than the full CSI exchange method [14], we thus utilize this method to solve problem (P2). Then, variables at BS $b := (i_0 + 1 \bmod B) + 1$ at the $i_0 + 1$ -th iteration can be updated by

$$\boldsymbol{\gamma}^{i_0+1} := \arg \min_{\boldsymbol{\gamma}} \mathcal{L}(\Theta^{i_0}, \mathbf{W}^{i_0}, \boldsymbol{\gamma}, \boldsymbol{\xi}^{i_0}, \boldsymbol{\lambda}^{i_0}), \quad (7a)$$

$$\boldsymbol{\xi}^{i_0+1} := \arg \min_{\boldsymbol{\xi}} \mathcal{L}(\Theta^{i_0}, \mathbf{W}^{i_0}, \boldsymbol{\gamma}^{i_0+1}, \boldsymbol{\xi}, \boldsymbol{\lambda}^{i_0}), \quad (7b)$$

$$\mathbf{w}_b^{i_0+1} := \arg \min_{\mathbf{w}_b} \mathcal{L}(\Theta^{i_0}, \mathbf{w}_b, \bar{\mathbf{w}}_b^{i_0}, \boldsymbol{\gamma}^{i_0+1}, \boldsymbol{\xi}^{i_0+1}, \boldsymbol{\lambda}^{i_0}), \quad (7c)$$

$$\theta_b^{i_0+1} := \arg \min_{\theta_b} \mathcal{L}(\theta_b, \bar{\theta}_b^{i_0}, \mathbf{W}^{i_0+1}, \boldsymbol{\gamma}^{i_0+1}, \boldsymbol{\xi}^{i_0+1}, \boldsymbol{\lambda}^{i_0}), \quad (7d)$$

$$\boldsymbol{\lambda}^{i_0+1} := \boldsymbol{\lambda}^{(i_0)} + \rho \sum_{b \in \mathcal{B}} \mathbf{A}_b \theta_b^{i_0+1}, \quad (7e)$$

where $\bar{\mathbf{w}}_b = \mathbf{W} \setminus \mathbf{w}_b$ and $\bar{\theta}_b = \Theta \setminus \theta_b$. Note, there are local copies of $\boldsymbol{\gamma}, \boldsymbol{\xi}$ and $\boldsymbol{\lambda}$ in each BS and they are updated locally.

In what follows, we focus on solving problems (7a)-(7d) and the iteration index is dropped to simplify notation. We first derive the optimal solutions of problems (7a)-(7c) in the following proposition.

Proposition 1: The optimal solution $\boldsymbol{\gamma}^*$ for problem (7a) is

$$\gamma_k^* = \Gamma_k, \quad k \in \mathcal{K}. \quad (8)$$

The optimal solution $\boldsymbol{\xi}^*$ for problem (7b) is

$$\xi_k^* = \frac{(\varphi_{k,k} + \psi_{k,k})\sqrt{(1 + \gamma_k)\omega_k}}{\sum_{j \in \mathcal{K}} |\varphi_{k,j} + \psi_{k,j}|^2 + \delta^2}, \quad k \in \mathcal{K}, \quad (9)$$

where $\psi_{k,j} = \sum_{b \in \mathcal{B}} \theta_b^H \mathbf{V}_k^H \mathbf{G}_b \mathbf{w}_{b,j}$ and $\varphi_{k,j} = \sum_{b \in \mathcal{B}} \mathbf{h}_{b,k}^H \mathbf{w}_{b,j}$.

Then, the optimal solution \mathbf{w}_b^* for problem (7c) is

$$\mathbf{w}_{b,k}^* = (\Phi_b + \mu_b \mathbf{I}_{N_t})^{-1} (\sqrt{(1 + \gamma_k)\omega_k} \xi_k^* \hat{\mathbf{h}}_{b,k}^H - \Omega_{b,k}), \quad \forall k, \quad (10)$$

where $\Omega_{b,k} = \sum_{j \in \mathcal{K}} |\xi_j|^2 \mathbf{w}_{l,k} \hat{\mathbf{h}}_{b,j}^H (\varphi_{j,k} + \psi_{j,k} - \hat{\mathbf{h}}_{b,j}^H \mathbf{w}_{b,k})$, $\Phi_b = \sum_{j \in \mathcal{K}} |\xi_j|^2 \hat{\mathbf{h}}_{b,j} \hat{\mathbf{h}}_{b,j}^H$, $\mu_b, \forall b$, can be obtained via bisection methods.

Proof: γ_k^* in (8), ξ_k^* in (9) and $\mathbf{w}_{b,k}^*$ in (10) can be obtained by respectively solving the following equations: $\frac{\partial \mathcal{L}(\Theta, \mathbf{W}, \boldsymbol{\gamma}, \boldsymbol{\xi}, \boldsymbol{\lambda})}{\partial \gamma_k} = 0$, $\frac{\partial \mathcal{L}(\Theta, \mathbf{W}, \boldsymbol{\gamma}, \boldsymbol{\xi}, \boldsymbol{\lambda})}{\partial \xi_k} = 0$ and $\frac{\partial \mathcal{L}(\Theta, \mathbf{W}, \boldsymbol{\gamma}, \boldsymbol{\xi}, \boldsymbol{\lambda})}{\partial \mathbf{w}_{b,k}} = 0$. ■

Then, we will propose an efficient method to solve problem (7d). To locally optimize θ_b at BS b , we first rewrite the augmented Lagrangian in (6) as

$$\begin{aligned} \mathcal{L}(\Theta, \mathbf{W}, \boldsymbol{\gamma}, \boldsymbol{\xi}, \boldsymbol{\lambda}) = & f(\Theta, \mathbf{W}, \boldsymbol{\gamma}, \boldsymbol{\xi}) + \sum_{b \in \mathcal{B}} \mathbb{1}_{\mathcal{F}}(\theta_b) + \frac{\rho}{2} \left\| \mathbf{A}_b \theta_b + \mathbf{t}_b + \frac{\boldsymbol{\lambda}}{\rho} \right\|^2 + C_1, \\ = & \theta_b^H \mathbf{Z} \theta_b - 2\text{Re}\{\theta_b^H \mathbf{q}\} + \mathbb{1}_{\mathcal{F}}(\theta_b) + C_1 + C_2, \quad (11) \end{aligned}$$

where $\mathbf{t}_b = \sum_{l \in \mathcal{B} \setminus b} \mathbf{A}_l \theta_l$, $\mathbf{Z} = \sum_{k \in \mathcal{K}} \sum_{j \in \mathcal{K}} \omega_k |\xi_j|^2 \mathbf{x}_{j,k} \mathbf{x}_{j,k}^H + \frac{\rho}{2} \mathbf{A}_b^H \mathbf{A}_b$, $\mathbf{x}_{j,k} = \text{diag}(\mathbf{v}_j^H) \mathbf{G}_b \mathbf{w}_{b,k}$,

$$\begin{aligned} \mathbf{q} = & \sum_{k \in \mathcal{K}} \sum_{j \in \mathcal{K}} \omega_k |\xi_j|^2 \mathbf{x}_{j,k} (\hat{\mathbf{h}}_{b,j}^H \mathbf{w}_{b,k} - \varphi_{j,k} - \psi_{j,k}) \\ & + \sum_{k \in \mathcal{K}} \omega_k \sqrt{1 + \gamma_k} \mathbf{x}_{k,k} - \frac{\rho}{2} \mathbf{A}_b^H (\mathbf{t} + \frac{\boldsymbol{\lambda}}{\rho}), \quad (12) \end{aligned}$$

and $C_{\{1,2\}}$ are constant terms, which are not related to θ_b . Thus, problem (7d) can be rewritten as

$$\min_{\theta_b} g_b(\theta_b) = \theta_b^H \mathbf{Z} \theta_b - 2\text{Re}\{\theta_b^H \mathbf{q}\}, \quad \text{s. t. } \theta_b \in \mathcal{F}. \quad (13)$$

Though problem (13) can be approximatively solved with the SDR technique [9], [15], finding the solution is of high complexity when NR is large (i.e., $O((NR+1)^{4.5})$ [15]). Based on our previous work [16], the MM method is an effective and low-complexity way to solve the non-convex problem (P4). The basic idea is to transform the original problem (13) into a sequence of majorized subproblems that can be solved with closed-form minimizers. At first, according to lemma 1 in [16], we can find a valid majorizer of $g_b(\theta_b)$ at point $\theta_b^{i_1} \in \mathcal{F}$ given by $g_b(\theta_b; \theta_b^{i_1}) = 2\text{Re}\{\theta_b^H ((\mathbf{Z} - \zeta \mathbf{I}) \theta_b^{i_1} - \mathbf{q})\} + C_3$, where C_3 is a constant term, ζ is the maximum eigenvalue of matrix \mathbf{Z} . Then, according to the MM method and utilizing the majorizer $g_b(\theta_b; \theta_b^{i_1})$, the solution of problem (13) can be obtained by iteratively solving the following problem

$$\min_{\theta_b} g_b(\theta_b; \theta_b^{i_1}), \quad \text{s. t. } \theta_b \in \mathcal{F}. \quad (14)$$

The closed-form solution for (14) is

$$\theta_b^{i_1+1} = -\exp(j\angle((\mathbf{Z} - \zeta \mathbf{I}) \theta_b^{i_1} - \mathbf{q})). \quad (15)$$

The proof of convergence for the MM method is similar to [16] and omitted here because of the space limitation. We define the stopping criteria of the MM method as $i_1 = I_1$, where I_1 is the maximum permitted number of iteration.

With the above analysis, we summarize the proposed fully decentralized beamforming scheme in Algorithm 1 (Algorithm 1). In Algorithm 1, the BSs are activated in a fixed sequencing order and all variables are incrementally updated. According to steps 6 and 18 in Algorithm 1, the required signaling information for local variables update at each BS includes one $NR|\mathcal{E}|$ -dimensional vector \mathbf{t} and two

Algorithm 1 Decentralized Beamforming Algorithm

1: **Input:** $\mathbf{h}_{b,k}, \mathbf{V}_k, \mathbf{G}_b, \mathbf{A}_b, \forall b, k$;
2: **Output:** $\mathbf{w}_{b,k}, \boldsymbol{\theta}_b, \forall b, k$;
3: **Initialize:** $\mathbf{w}_{b,k}^0, \boldsymbol{\theta}_b^0, \forall b, k, \lambda^0$;
4: **for** $i_0 = 0, 1, \dots$ **do**
5: BS $b: = b_{i_0} = (i_0 \bmod B) + 1$ **do**:
6: **receive** $\mathbf{t}^{i_0}, \boldsymbol{\varphi}^{i_0}$ and $\boldsymbol{\psi}^{i_0}$.
7: **update** $\mathbf{t}_b^{i_0+1} = \mathbf{t}^{i_0} - \mathbf{A}_b \boldsymbol{\theta}_b^{i_0}$;
8: **update** $\bar{\varphi}_{k,j}^{i_0+1} = \varphi_{k,j}^{i_0} - \mathbf{h}_{b,k} \mathbf{w}_{b,j}^{i_0}, k, j \in \mathcal{K}$;
9: **update** $\bar{\psi}_{k,j}^{i_0+1} = \psi_{k,j}^{i_0} - \boldsymbol{\theta}_b^{i_0 H} \mathbf{V}_k^H \mathbf{G}_b \mathbf{w}_{b,j}^{i_0}, k, j \in \mathcal{K}$;
10: **update** $\gamma_k^{i_0+1}, \forall k$, using (8);
11: **update** $\xi_k^{i_0+1}, \forall k$, using (9);
12: **update** $\mathbf{w}_{b,k}^{i_0+1}, \forall k$, using (10);
13: **update** $\boldsymbol{\theta}_b^{i_0+1}$ by solving problem (7d);
14: **update** λ^{i_0+1} using (7e);
15: **update** $\mathbf{t}^{i_0+1} = \mathbf{t}_b^{i_0+1} + \mathbf{A}_b \boldsymbol{\theta}_b^{i_0+1}$;
16: **update** $\varphi_{k,j}^{i_0+1} = \bar{\varphi}_{k,j}^{i_0+1} + \mathbf{h}_{b,k} \mathbf{w}_{b,j}^{i_0+1}, k, j \in \mathcal{K}$;
17: **update** $\psi_{k,j}^{i_0+1} = \bar{\psi}_{k,j}^{i_0+1} + \boldsymbol{\theta}_b^{i_0+1 H} \mathbf{V}_k^H \mathbf{G}_b \mathbf{w}_{b,j}^{i_0+1}, k, j \in \mathcal{K}$;
18: **send** $\mathbf{t}^{i_0+1}, \boldsymbol{\varphi}^{i_0+1}$ and $\boldsymbol{\psi}^{i_0+1}$ to BS b_{i_0+1} .
19: **until** the stopping criterion is met.
20: **end for**

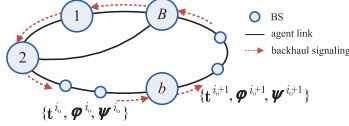
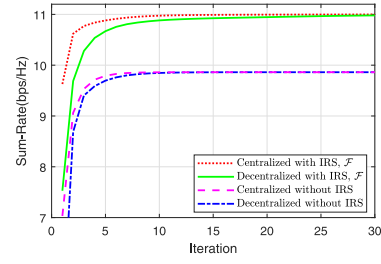


Fig. 2. Example for the update of Algorithm 1.

$K \times K$ -dimensional matrices, i.e., $\boldsymbol{\varphi}$ and $\boldsymbol{\psi}$. Then, \mathbf{t} , $\boldsymbol{\varphi}$ and $\boldsymbol{\psi}$ are incrementally updated (as shown in steps 7-9 and 15-17 in Algorithm 1) and transmitted to the next BS after updating local \mathbf{w}_b and $\boldsymbol{\theta}_b$. To facilitate understanding how the BSs exchange the signaling information, an example of Algorithm 1 is shown in Fig. 2. Note that, we do not have to exchange all CSI among BSs in each iteration, and the signaling overhead does not depend on the number of transmit antennas and channels. The total required backhaul signaling of the proposed scheme at each iteration is $B(2K^2 + NR|\mathcal{E}|)$ symbols. Thus, the proposed scheme can significantly reduce signaling when compared with full CSI and updated variables exchange among BSs. Until Algorithm 1 converges, the BSs send $\boldsymbol{\theta}_b, \forall b$ back to the IRS controller. We then analyze the convergence and complexity of Algorithm 1 in the following proposition.

Proposition 2: The sequence $(\boldsymbol{\Theta}^{i_0}, \mathbf{W}^{i_0}, \boldsymbol{\gamma}^{i_0}, \boldsymbol{\xi}^{i_0}, \lambda^{i_0})$ generated by Algorithm 1 can converge to a stationary point $(\boldsymbol{\Theta}^*, \mathbf{W}^*, \boldsymbol{\gamma}^*, \boldsymbol{\xi}^*, \lambda^*)$ of \mathcal{L} , i.e., $0 \in \partial \mathcal{L}(\boldsymbol{\Theta}^*, \mathbf{W}^*, \boldsymbol{\gamma}^*, \boldsymbol{\xi}^*, \lambda^*)$. When the MM method is used, the main complexity in each iteration of Algorithm 1 is $O(KBN_t^3 + B((NR)^3 + I_t(NR)^2))$.

Proof: According to the general convergence proof for the ADMM method w.r.t. non-convex problems in [17], we can find that the objective function of (P2) is continuous and the feasible set \mathcal{F} is bounded, as well as the Lipschitz sub-minimization path conditions in [17] are met. Thus, based on in [17, Th. 2], we conclude that Algorithm 1 can converge to a stationary point $(\boldsymbol{\Theta}^*, \mathbf{W}^*, \boldsymbol{\gamma}^*, \boldsymbol{\xi}^*, \lambda^*)$ of \mathcal{L} . Although the

Fig. 3. Sum-rate vs the number of iterations, with $N_t = 25, N = 16$.

duality gap may be non-zero, Algorithm 1 still converges and in general the dual function at the convergence point is a lower bound of the optimal value of problem (P2).

In each iteration of Algorithm 1, the main complexity is the inversion operation in (10) and finding the maximum eigenvalue of \mathbf{Z} when using the MM method to solve problem (7d), which lead to the complexity of $O(N_t^3)$ and $O((NR)^3)$, respectively. ■

The centralized beamforming scheme, where all beamformers are computed by the CPU of cell-free networks, can be derived following a similar procedure to [10]. For more practical implementation of IRSs, low-resolution discrete phase shifts should be considered, i.e., $[\boldsymbol{\theta}]_i \in \mathcal{F}_2 = \{e^{j2\pi u/2^U} | u = 0, \dots, 2^U - 1\}$, where the resolution of phase shift is controlled by U bits. Then, according to the nearest point projection in [10], the solution of (P5) w.r.t. $[\boldsymbol{\theta}_b]_i \in \mathcal{F}_2$ can be obtained by solving problem $\angle[\boldsymbol{\theta}_b]_i^* = \arg \min_{[\boldsymbol{\theta}_b]_i \in \mathcal{F}_2} |\angle[\boldsymbol{\theta}_b]_i - \angle[\boldsymbol{\theta}_b]_i^o|$, where $[\boldsymbol{\theta}_b]_i^o$ is the solution with the MM method.

IV. NUMERICAL RESULTS

In this section, numerical results are provided to evaluate the effectiveness of the proposed algorithm. To evaluate the average network performance, we simulate 100 network realizations. In each realization, we consider the scenario where BSs are located on a circle centered at $(0, 0)$ with radius D , and IRSs and UEs are randomly distributed in this circle. Meanwhile, due to the mobility of UEs, each link (i.e., BS-UE, BS-IRS, or IRS-UE link) is a random non-line-of-sight (NLOS) link or line-of-sight (LOS) link. For large-scale fading, the distance-wavelength-dependent pathloss is given by $PL(d) = \epsilon d^{-\alpha}$, where d is distance, ϵ is a carrier frequency dependent constant and α is the pathloss exponent. For small-scale fading, we assume that the NLOS link is modeled by Rayleigh fading, while the LOS link is modeled by Rician fading with Rician factor 0 dB [10]. The bandwidth is 1 GHz with central carrier frequency 28 GHz. Then, we have $\epsilon = -61.3$ dB and the pathloss exponent for the NLOS (LOS) link is 3.2 (2.1) according to [7]. To facilitate illustration, we set $\omega_k = 1, \forall k, P_b = P_t = 0$ dBm, $\forall b, B = 4, K = 4, R = 3, I_{\text{in}} = 50$ and $D = 50$ m.

Fig. 3 presents the convergence of the proposed algorithm. For the case without IRSs, we see that both decentralized and centralized method can converge very fast (i.e., within 10 iterations). For the case with IRSs, since there is a consensus constraint w.r.t. the beamformers of IRSs, it is shown that the convergence rate of the decentralized method is lower than that of centralized methods. For example, the centralized method can converge within 20 iterations, while the decentralized method can converge within 30 iterations. For the cases with and without IRSs, the decentralized method can converge

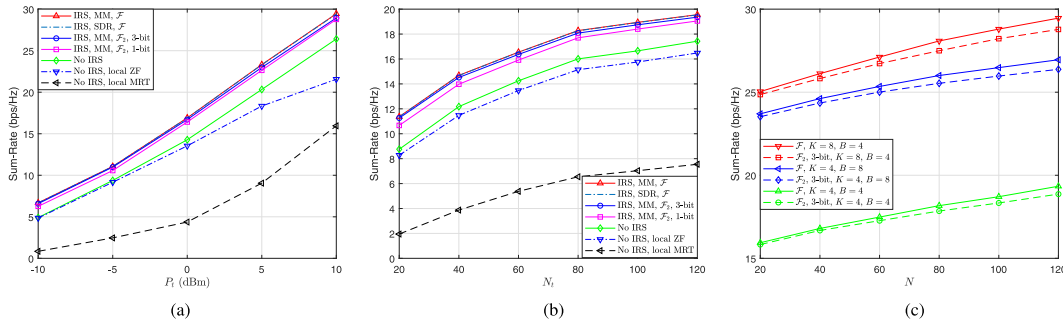


Fig. 4. Sum-rate of decentralized beamforming methods vs: (a) P_t with $N_t = 64$, $N = 36$; (b) N_t with $N = 36$; (c) N with $N_t = 64$.

to the same sum-rate as the centralized method. The result verifies the effectiveness of the proposed method.

Fig. 4 shows the achievable sum-rate of various decentralized beamforming methods versus P_t , N_t , K , B and N . Fig. 4(a) shows that the sum-rate of proposed decentralized beamforming methods increases with P_t , and outperforms that of local ZF and MRT methods. The system with the aid of IRSs can achieve a higher sum-rate than that without IRSs. Moreover, the low-resolution phase shifts suffer acceptable performance loss. For instance, the system with “1-bit” phase shifts suffers the sum-rate loss of 3.8% of that with continuous phase shifts. From Fig. 4(b), we can see that the sum-rate of all beamforming methods increases with N_t . The sum-rate of proposed decentralized beamforming methods still outperforms that of local ZF and MRT methods. Fig. 4(a) and Fig. 4(b) show that the MM method can achieve comparable performance to the SDR method. Fig. 4(c) shows the sum-rate of proposed decentralized beamforming methods versus K , B and N . It is shown that the sum-rate increases with K , B , and N . Moreover, by doubling N , the sum-rate increases almost 1 bps/Hz. However, as N and K increases, the sum-rate gap between low-resolution phase shifts and continuous phase shifts increases.

V. CONCLUSION

We have developed a decentralized design framework for cooperative beamforming in IRS-aided cell-free networks. Based on incremental ADMM methods, a fully decentralized beamforming scheme has been proposed to locally update beamformers, in which both transmitting digital beamformers and IRS-based analog beamformers are jointly optimized. The convergence of the proposed method has been proven and the main complexity has been analyzed. Results show that the proposed method for the cases with and without IRSs can achieve better performance than existing decentralized methods (i.e., local MRT and ZF methods). Moreover, it has been shown that IRS-aided cell-free networks outperform conventional cell-free networks, and that the system sum-rate increases with the number of transmit antennas and the size of IRSs. Finally, we have seen that, to achieve acceptable performance loss, the quantization level of phase shifts is related to the size of IRSs and the number of antennas.

REFERENCES

- [1] S. Buzzi and C. D’Andrea, “Cell-free massive MIMO: User-centric approach,” *IEEE Wireless Commun. Lett.*, vol. 6, no. 6, pp. 706–709, Dec. 2017.
- [2] T. C. Mai, H. Q. Ngo, and T. Q. Duong, “Downlink spectral efficiency of cell-free massive MIMO systems with multi-antenna users,” *IEEE Trans. Commun.*, vol. 68, no. 8, pp. 4803–4815, Aug. 2020.
- [3] H. Q. Ngo, A. Ashikhmin, H. Yang, E. G. Larsson, and T. L. Marzetta, “Cell-free massive MIMO versus small cells,” *IEEE Trans. Wireless Commun.*, vol. 16, no. 3, pp. 1834–1850, Mar. 2017.
- [4] G. Interdonato, M. Karlsson, E. Björnson, and E. G. Larsson, “Local partial zero-forcing precoding for cell-free massive MIMO,” *IEEE Trans. Wireless Commun.*, vol. 19, no. 7, pp. 4758–4774, Jul. 2020.
- [5] E. Nayeibi, A. Ashikhmin, T. L. Marzetta, H. Yang, and B. D. Rao, “Precoding and power optimization in cell-free massive MIMO systems,” *IEEE Trans. Wireless Commun.*, vol. 16, no. 7, pp. 4445–4459, Jul. 2017.
- [6] I. Atzeni, B. Gouda, and A. Tölili, “Distributed precoding design via over-the-air signaling for cell-free massive MIMO,” 2020. [Online]. Available: arXiv:2004.00299.
- [7] T. S. Rappaport, Y. Xing, G. R. MacCartney, A. F. Molisch, E. Mellios, and J. Zhang, “Overview of millimeter wave communications for fifth-generation (5G) wireless networks—With a focus on propagation models,” *IEEE Trans. Antennas Propag.*, vol. 65, no. 12, pp. 6213–6230, Dec. 2017.
- [8] E. Björnson, Ö. Özdogan, and E. G. Larsson, “Intelligent reflecting surface versus decode-and-forward: How large surfaces are needed to beat relaying?” *IEEE Wireless Commun. Lett.*, vol. 9, no. 2, pp. 244–248, Feb. 2020.
- [9] C. You, B. Zheng, and R. Zhang, “Channel estimation and passive beamforming for intelligent reflecting surface: Discrete phase shift and progressive refinement,” *IEEE J. Sel. Areas Commun.*, vol. 38, no. 11, pp. 2604–2620, Nov. 2020.
- [10] Z. Zhang and L. Dai, “A joint precoding framework for wideband reconfigurable intelligent surface-aided cell-free network,” 2020. [Online]. Available: arXiv:2002.03744.
- [11] H. Alwazani, A. Kammoun, A. Chaaban, M. Debbah, and M.-S. Alouini, “Intelligent reflecting surface-assisted multi-user MISO communication: Channel estimation and beamforming design,” *IEEE Open J. Commun. Soc.*, vol. 1, pp. 661–680, 2020.
- [12] K. Shen, W. Yu, L. Zhao, and D. P. Palomar, “Optimization of MIMO device-to-device networks via matrix fractional programming: A minorization-maximization approach,” *IEEE/ACM Trans. Netw.*, vol. 27, no. 5, pp. 2164–2177, Oct. 2019.
- [13] Y. Ye, M. Xiao, and M. Skoglund, “Mobility-aware content preference learning in decentralized caching networks,” *IEEE Trans. Cogn. Commun. Netw.*, vol. 6, no. 1, pp. 62–73, Mar. 2020.
- [14] Y. Ye, H. Chen, Z. Ma, and M. Xiao, “Decentralized consensus optimization based on parallel random walk,” *IEEE Commun. Lett.*, vol. 24, no. 2, pp. 391–395, Feb. 2020.
- [15] Y. Yang, B. Zheng, S. Zhang, and R. Zhang, “Intelligent reflecting surface meets OFDM: Protocol design and rate maximization,” *IEEE Trans. Commun.*, vol. 68, no. 7, pp. 4522–4535, Jul. 2020.
- [16] S. Huang, Y. Ye, and M. Xiao, “Learning based hybrid beamforming design for full-duplex millimeter wave systems,” *IEEE Trans. Cogn. Commun. Netw.*, early access, Aug. 26, 2020, doi: 10.1109/TCCN.2020.3019604.
- [17] Y. Wang, W. Yin, and J. Zeng, “Global convergence of ADMM in nonconvex nonsmooth optimization,” *J. Sci. Comput.*, vol. 78, no. 1, pp. 29–63, 2019.